



Dynamical behavior of the multiplicative diffusion coupled map lattices

Wei Wang and Hilda A. Cerdeira

Citation: *Chaos: An Interdisciplinary Journal of Nonlinear Science* **6**, 200 (1996); doi: 10.1063/1.166165

View online: <http://dx.doi.org/10.1063/1.166165>

View Table of Contents: <http://scitation.aip.org/content/aip/journal/chaos/6/2?ver=pdfcov>

Published by the [AIP Publishing](#)

Articles you may be interested in

[Integrable discretizations of the Bogoyavlensky lattices](#)

J. Math. Phys. **37**, 3982 (1996); 10.1063/1.531611

[Controlling spatiotemporal chaos in one and twodimensional coupled logistic map lattices](#)

AIP Conf. Proc. **375**, 104 (1996); 10.1063/1.51021

[Kink dynamics in onedimensional coupled map lattices](#)

Chaos **5**, 602 (1995); 10.1063/1.166129

[Clustering motion in conservative coupled map systems](#)

AIP Conf. Proc. **256**, 571 (1992); 10.1063/1.42397

[Recurrence of KAM tori and their novel critical behavior in nonanalytic twist maps](#)

AIP Conf. Proc. **248**, 177 (1992); 10.1063/1.41942



Dynamical behavior of the multiplicative diffusion coupled map lattices

Wei Wang

National Laboratory of Solid State Microstructure, Institute of Solid State Physics, and Physics Department
Nanjing University, Nanjing 210093, People's Republic of China and Center of Advanced Science
and Technology in Solid State Physics, Nanjing 210093, People's Republic of China

Hilda A. Cerdeira

The International Center for Theoretical Physics, P.O. Box 586, 34100 Trieste, Italy

(Received 1 October 1993; accepted for publication 12 September 1995)

We report a dynamical study of multiplicative diffusion coupled map lattices with the coupling between the elements only through the bifurcation parameter of the mapping function. We discuss the diffusive process of the lattice from an initially random distribution state to a homogeneous one as well as the stable range of the diffusive homogeneous attractor. For various coupling strengths we find that there are several types of spatiotemporal structures. In addition, the evolution of the lattice into chaos is studied. A largest Lyapunov exponent and a spatial correlation function have been used to characterize the dynamical behavior. © 1996 American Institute of Physics.

[S1054-1500(96)00401-2]

I. INTRODUCTION

Phenomena with spatiotemporal complexity are common in nature and can be observed in fluid, chemical, optical, and solid-state turbulence, pattern formation, neural networks, parallel computation problems, and so on. For example, turbulent flows, chemical reactions with diffusion, spin wave turbulence, and biological networks are some complex phenomena which can display chaotic dynamics. These systems must be described by taking into account spatial variables, and in recent years exciting studies on spatiotemporal chaos have been performed.¹⁻⁹ Spiral waves are also presented in some interesting biological phenomena as morphogenesis or in brain dynamics.¹⁰ In some cases they become unstable giving rise to turbulent (chaotic) behavior from an initially well-defined spatially ordered state. A strange attractor can be obtained then by calculating the time evolution of the given variables in concrete points of the space domain. On the other hand, many dynamical properties have been explored with coupled map lattice models. Phase transitions, chaotic strings, intermittency, turbulence, and other phenomena have been particularly well characterized.^{6-8,11-13}

It is well known that some nonlinear continuous models based on reaction diffusions can give spatial structures through Turing symmetry-breaking instabilities and it seems an evident step to consider an equivalent approach based on the coupled map lattice theory.¹⁴ The coupled map lattice which has been studied intensively during the last years is a dynamical system with a discrete time, discrete space, and continuous state. There are many one-dimensional models which can be given by

$$x_{n+1}(i) = \alpha f(x_n(i)) + \beta g[f(x_n(i)), f(x_n(i+1)), f(x_n(i-1))], \quad (1)$$

where the function g can, for instance, be chosen as the diffusive coupling

$$g = f(x_n(i+1)) + f(x_n(i-1)) - 2f(x_n(i)); \quad (2)$$

one-way coupling

$$g = f(x_n(i)) - f(x_n(i-1)); \quad (3)$$

also, models with global coupling have been studied,

$$g = \sum_{j=1}^N f(x_n(j)), \quad (4)$$

and so on. For the logistic mapping function, $f = 1 - Ax^2$, a complex dynamical behavior has been found which contains: period doubling of kink-antikink pattern; zigzag patterns (or antiferro-like structures); spatiotemporal intermittency: burst and laminar regions from complicated spatiotemporal patterns; and spatial amplification of noise.^{6,7,11} However, all of these models are too simple to discuss the dynamical behavior of a real system although one still hopes that some of the novel features are useful to understanding the behavior of many different systems.⁷

In this work, we present a dynamical study of multiplicative diffusion coupled map lattices where the coupling between the elements is chosen only through the bifurcation parameter of the mapping function. Our aim here is to discuss the diffusive process of the coupled map lattices from an initially random distribution state to a homogeneous one, and to study the spatiotemporal structures and the dynamical behavior of the system when the coupling parameter varies over some ranges. In addition, we are also interested in finding how the system develops into chaos when the coupling is increased. The organization of this paper is as follows. In Sec. II, we present the model as well as a simple analytical treatment of the diffusive process. Then we demonstrate the spatiotemporal structures of the lattice and discuss the statistical property and the spatial correlation in Sec. III. In Sec. IV, to characterize the dynamical behavior of the lattice, we calculate the largest Lyapunov exponent. Finally, we give the conclusions in the last section.

II. SPATIOTEMPORAL STRUCTURES OF THE MULTIPLICATIVE DIFFUSION COUPLED MAP LATTICES

A. Model

The state of any element with discrete coordinate j at the time moment n of the multiplicative diffusion coupled map lattices (here we only consider the one-dimensional case) is characterized by the variable $x_n(j)$. Evolution of the state of the lattices as a function of the discrete time step n is specified by the map

$$x_{n+1}(j) = f[x_n(j), D_n(x_n(j))], \quad (5)$$

where $D_n(x_n(j)) = D_0 + D \partial^2 x_n(j)$ represents the bifurcation parameter of the mapping and the coupling between the elements is given by

$$\partial^2 x_n(j) = \frac{1}{2}[x_n(j+1) + x_n(j-1) - 2x_n(j)], \quad (6)$$

and D_0 is the bifurcation parameter in the absence of coupling, i.e., D_0 corresponds to the bifurcation parameter without spatial correlation, and D is the coefficient of the coupling between the elements.¹⁵

For simplicity, we choose the mapping function $f(x)$ to be the logistic map

$$f(x) = \mu x(1-x). \quad (7)$$

Thus, the model becomes

$$x_{n+1}(j) = [D_0 + D \partial^2 x_n(j)] x_n(j) [1 - x_n(j)], \quad (8)$$

with the coupling parameter defined by Eq. (6).

From Eq. (8), we can see that if the correlation in space is zero ($D=0$), the dynamical state of the lattices depends simply on the single logistic map with the well-known period-doubling route to chaos as the parameter D_0 is increased. It means that the lattice consists of a set of independent elements. This is a trivial case in the present study. However, as long as $D \neq 0$, the state of the lattice not only depends on the coupling, but also on the value of D_0 . In this paper, we restrict ourselves to the case $1 < D_0 < 3$, for example, $D_0 = 2.9$, for which value the logistic map $x_{n+1} = D_0 x_n (1 - x_n)$ has only a stable fixed point $x^* = 1 - 1/D_0$. However, in our coupled lattice, we will have several types of spatiotemporal structures for different values of D due to the coupling between the elements as discussed in Sec. II B.

This multiplicative diffusion coupled map lattice can be used as a simple model for the reaction–diffusion process. It can be considered as a coarse discretion of the reaction–diffusion equation, which governs the growing phase

$$\frac{\partial x}{\partial t} = f \frac{\partial^2 x}{\partial r^2} + v(x), \quad (9)$$

where the coefficient $f = f[x(r,t)]$ depends on the state of the system $x(r,t)$ and, thus, varies both in space and time, and $v(x)$ is the velocity of growth. When $v(x) = 0$ Eq. (9) describes the crystal growth for a supercooled liquid.¹⁶ In a recent paper Ben-Jacob *et al.*¹⁷ studied the interfacial pattern formation during diffusion-limited growth of *Bacillus subtilis*,

they proposed a phase-field-like model (the phase being the bacterial concentration and the field being the nutrient concentration) to describe the growth. The bacteria–bacteria interaction is manifested as a phase-dependent diffusion constant, $D(\phi)$, in their model:

$$\frac{\partial \phi}{\partial t} = D(\phi) \nabla^2 \phi + g(\phi, c), \quad (10)$$

which is a higher-dimensional version of Eq. (9). In addition, diffusing coupling appears also in cellular automata models of some chemical and biological systems, such as the biological populations with and without generation overlap if we consider a coupled model of multisubsystems. One should be aware, however, of the fact that the discretization of these continuous equations introduces new phenomena. In particular, the chaotic states found in a lattice mapping may not have the counterparts in the continuous space–time models. Also, it should be noticed that the analysis of stability based on a minimum wavelength, which will be presented in the next section, will not work for a continuous space dimension.

B. Diffusive homogeneous attractor and frozen phenomenon

Suppose an initial state with a random distribution, i.e., $x_0(j) \in (0,1)$ for $(j=1,N)$ where N is the size of the lattice. In the case of $1 < D_0 < 3$ after a number of iterations of Eq. (8), the lattice may reach a homogeneous state (or diffusion homogeneous state), $x_n(j) = x^*$ for $(j=1,N)$ with the value of D changing over some ranges. This entire stable diffusive homogeneous state is an attractor since it is a fixed point of the lattice. However, one can expect that as the coupling parameter $|D|$ increases, the local small deviation may destroy the stable state due to the influence of the coupling between the elements. Now let us consider the range of D and the stability of this state. For certain element, i th, the stability is determined by its small deviation ϵ_n^i from the fixed point x^* , $x_n(j) = x^* + \epsilon_n^j$. Then by substituting this equation into Eq. (8), we have

$$\epsilon_{n+1}^j = A \epsilon_n^j + B(\epsilon_n^{j+1} + \epsilon_n^{j-1}) \quad (11)$$

with

$$A = D_0(1 - 2x^*) - Dx^*(1 - x^*) \quad B = \frac{D}{2} x^*(1 - x^*). \quad (12)$$

In obtaining Eq. (11), we have only taken the first order of ϵ_n^j . In order to discuss the stability for various perturbations (all the wavelengths), we introduce a Fourier transform

$$\epsilon_n^j = \frac{1}{N} \sum_{k=1}^N e^{i2\pi(jk/N)} \alpha_n^k; \quad (13)$$

and

$$\alpha_n^k = \sum_{l=1}^N e^{-i2\pi(lk/N)} \epsilon_n^l \quad (14)$$

with the normalization condition

$$\frac{1}{N} \sum_{j=1}^N e^{i2\pi j[(k-k')/N]} = \delta_{k,k'}. \quad (15)$$

Then we have

$$\begin{aligned} \alpha_{n+1}^k &= A\alpha_n^k + 2B\alpha_n^k \cos(2\pi k/N) \\ &= [A + 2B \cos(2\pi k/N)]\alpha_n^k. \end{aligned} \quad (16)$$

Thus the stability condition for the state $x^* = 1 - 1/D_0$ reads

$$-1 < A + 2B \cos(2\pi k/N) < 1. \quad (17)$$

From Eq. (17), we know that the stability is governed by the two extreme behaviors: $\cos(2\pi k/N) = -1$ when $k = N/2$, the short wavelength case, and $\cos(2\pi k/N) = 1$ for $k = N$, the long wavelength case. For the short wavelength behavior we have

$$|A - 2B| < 1. \quad (18)$$

That is

$$-1 < 2 - D_0 - \frac{2D(D_0 - 1)}{D_0^2} < 1; \quad (19)$$

and for the long wavelength case we get

$$|A + 2B| < 1, \quad (20)$$

which finally becomes

$$1 < D_0 < 3. \quad (21)$$

When D_0 is chosen to be 2.9, we have

$$D_2 < D < D_1, \quad (22)$$

with $D_1 = 0.2213$ and $D_2 = -8.41$. In addition to the stability condition Eq. (17), there is another implicit one:

$$1 < D_0 + D\partial^2 x_n(j) < 3, \quad (23)$$

since we only discuss the diffusive homogeneous state of the lattice. For $0 < D < D_1$, Eq. (23) is always true. But for $D_2 < D < 0$, in some ranges of D Eq. (23) fails. It will be shown that the lower limit value of D , D_3 , for the existence of this diffusive homogeneous attractor is equal to -2.9 , i.e., $D_3 = -2.9$ (see following discussion). In our numerical iterations, we find that there is an excellent agreement for $D_1 = 0.2213$, the upper limit value for the lattice with a diffusive homogeneous attractor with the analytic result given by Eq. (22). When $D_3 < D < D_1$ the state of the lattice converges to the attractor $x_n(j) = x^*$ with $(j = 1, N)$. However, when $D_2 < D < D_3$, some sites have zero value of $x_n(j)$, $x_n(j) = 0$. We call this state the frozen phenomenon which is related to the breaking of Eq. (23), $D_0 + D\partial^2 x_n(j) > 3$. The onset value of D of the frozen phenomenon is just the lower limit value of D for the existence of the diffusive homogeneous attractor. The mechanism of this frozen phenomenon can be understood as follows. In order to determine the onset value of D of the freezing or the lower limit value of D for the diffusive homogeneous attractor, we assume that there is a freezing of certain site i to zero, $x_n(j) = 0$, while the neighbors are still on the diffusive

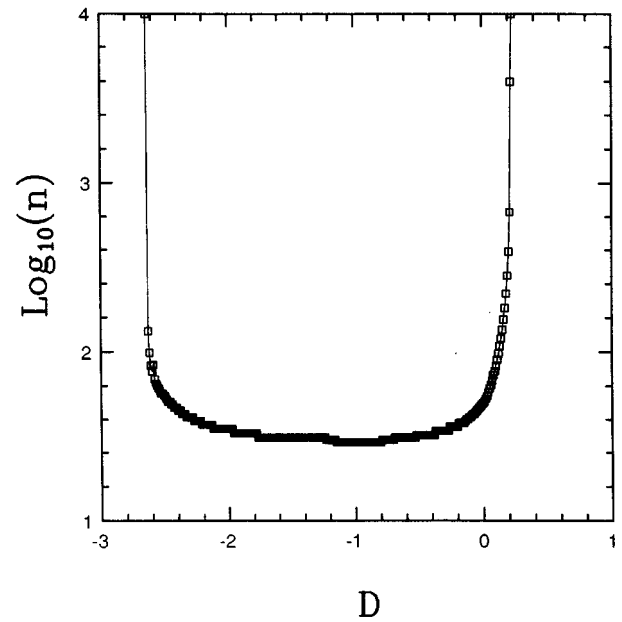


FIG. 1. The stable range of the diffusive homogeneous attractor in D parameter space for $D_0 = 2.9$ in Eq. (8).

homogeneous attractor, that is, $x_n(j+1) = x_n(j-1) = x^*$ and $x_n(j) = 0$. This gives $\partial^2 x_n(j) = x^*$ and from Eq. (14), then we have

$$D_0 + D\partial^2 x_n(j) = D_0 + Dx^* = 1. \quad (24)$$

Equation (24) gives the condition of the onset of $x_n(j)$ freezing to zero, $x_n(j) = 0$. From Eq. (24), one gets

$$D_3 = -D_0 = -2.9. \quad (25)$$

Finally, we conclude that the stable range of the diffusive homogeneous attractor is $D_3 < D < D_1$ and when $D < D_3$, the attractor is no longer stable and there is a frozen phenomenon, some sites attain zero value. On the other hand, when $D > D_1$, the attractor is also unstable and there will be a multistable state of $x_n(j)$ since Eq. (23) changes into $D_0 + D\partial^2 x_n(j) > 3$ and this corresponds to the case of bifurcation of the multiplicative diffusion coupled map lattices.

III. NUMERICAL ITERATIONS AND SPATIO-TEMPORAL STRUCTURES

A. Spatiotemporal patterns

We have made a numerical iteration of Eq. (8) by using an initially random distribution of $x_0(j) \in (0, 1)$ with $j = 1, N$. The size of the lattice is $N = 1000$ and a periodic boundary condition $x_n(N+1) = x_n(1)$ is also used in the present paper. In Fig. 1, we have shown the time steps or the number of iterations, n , with which the lattice reaches the diffusive homogeneous attractor, $x_n(j) = x^*$, $(j = 1, N)$ versus the coupling coefficient D and the stable range of this attractor. The criterion for the diffusive homogeneous attractor was such that the attractor was reached with $|x_n(j+1) - x_n(j)| < 10^{-4}$ for all sites of the lattice. From Fig. 1, we can see that when $-2.64 < D < 0.2212$, the finally stable state of the multiplica-

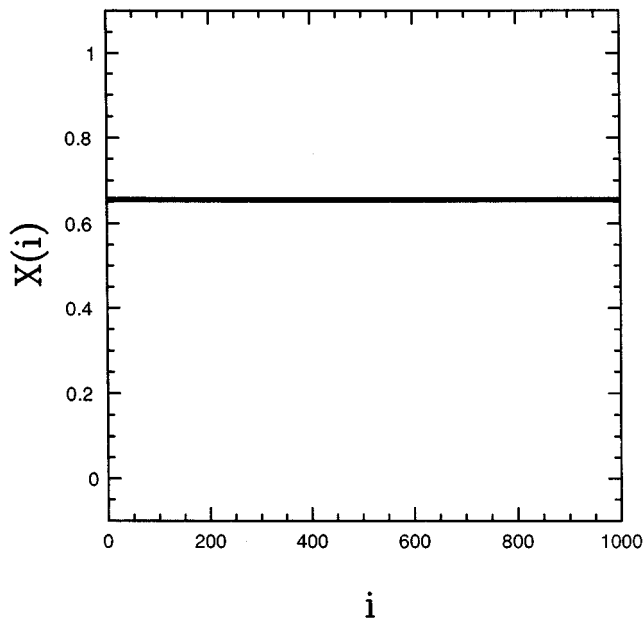


FIG. 2. The diffusive homogeneous attractor with $D_0=2.9$ and $D=-1.0$.

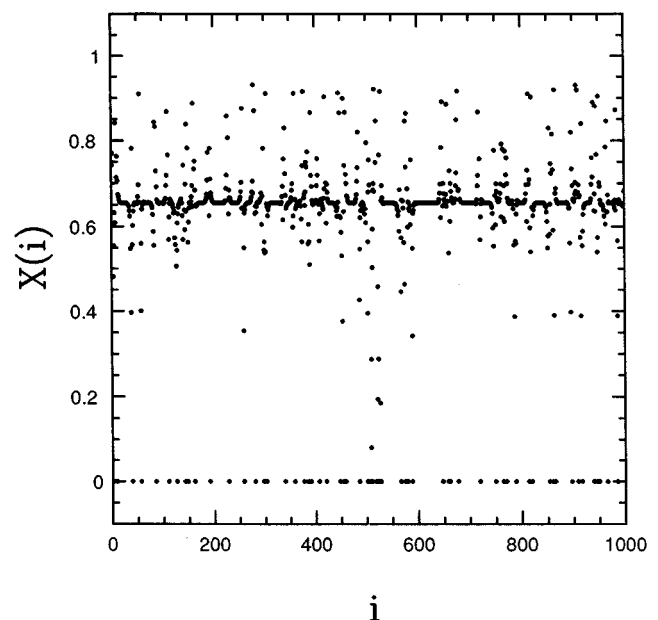


FIG. 3. A snapshot of the frozen phenomenon with $D_0=2.9$ and $D=-3.0$.

tive diffusion coupled map lattices is a diffusive homogeneous attractor, while for $D < -2.64$ and $D > 0.2212$, there exists no stable attractor for n up to 10^4 . On the bottom of this curve, the attractor is reached only after $n \sim 30$. In Fig. 1, we only study the spatiotemporal structures for $-4.0 < D < 3.2$ since we kept Eq. (8) to be in $(0,1)$.

In our iterations, we found that there are several types of the spatiotemporal structures, or patterns: (i) When $-2.64 < D < 0.2212$, the stable state is an attractor $x_n(j) = x^*$, the diffusive homogeneous attractor. Here we found that there is an excellent agreement with the previous discussion for the upper limit value, $D_1 = 0.2213$. But the lower limit value of D is not equal to -2.9 . This is because there is a more sensitive effect of the fluctuation of the system when D approaches $D_3 = -2.9$ and the fluctuation makes the onset of the frozen phenomenon occur earlier. An example of the diffusive homogeneous pattern is shown in Fig. 2. (ii) For $-4.0 < D < -2.64$, there exists a frozen phenomenon which is shown in Fig. 3. We have seen that there are many sites frozen to zero. The zeros divide the lattice into many domains or subsystems and correspond to placing many insulating walls in the lattice. These walls block the occurrence of diffusion in the lattice since the boundary conditions for these domains are fixed to zero. In a larger range of D values, the number of the zeros, M , is stable, unchanged. For small values of $|D|$, M , becomes stable within a short number of iterations. However, when $|D|$ is larger, the number of zeros stabilizes with a very long transient. The relation of the number of zeros with the coupling coefficient D is almost linear, $M \sim D$. In addition, we have seen that within the domains, the dynamical behavior is complex. Some domains are still on the attractor $x_n(j) = x^*$, some are chaotic. For example, a small part of the attractor is shown in Fig. 4. To get the figure, we have discarded 5000 iterations and plotted

1000 points for each site. From Fig. 4, we can see that the sites within a domain equally distant from the boundaries, zeros, undergo the same dynamical behavior. This means that the interaction model is spatially symmetric. In Fig. 5, we show a first return map for site $j=511$, we see that the dynamical state for this site is chaotic. The situation is the same for other sites either still on the diffusive homogeneous attractor or on the chaotic state. (iii) When $0.2212 < D < 1.215$, the pattern is a period-2 state. A bifurcation diagram for site $j=456$ is shown in Fig. 6(a). The period-2 state is stable over a large range of the D values. For $1.215 < D < 3.2$, the pattern undergoes a transition from a quasiperiodic to a chaotic state [see Fig. 6(a)]. We will discuss this in the following section. In addition, in Fig. 6(b) we have also shown the same diagram for the coupling function Eq. (6),

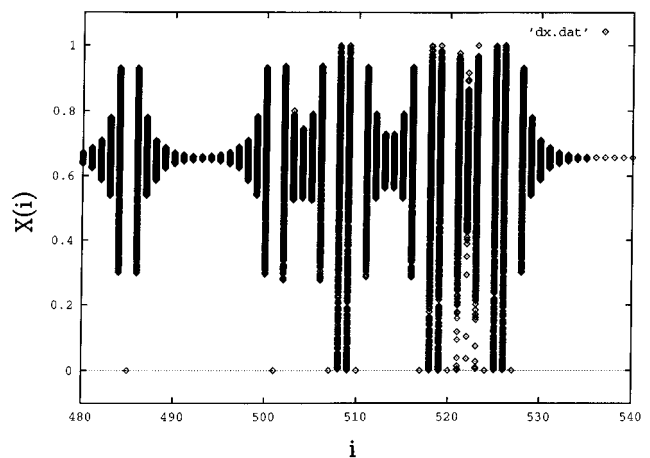


FIG. 4. A part of the attractor for sites $i=480-540$ of the lattice with $D_0=2.9$ and $D=-3.0$. 5000 iterations have been discarded and the following 1000 points have been plotted for each site of the lattice.

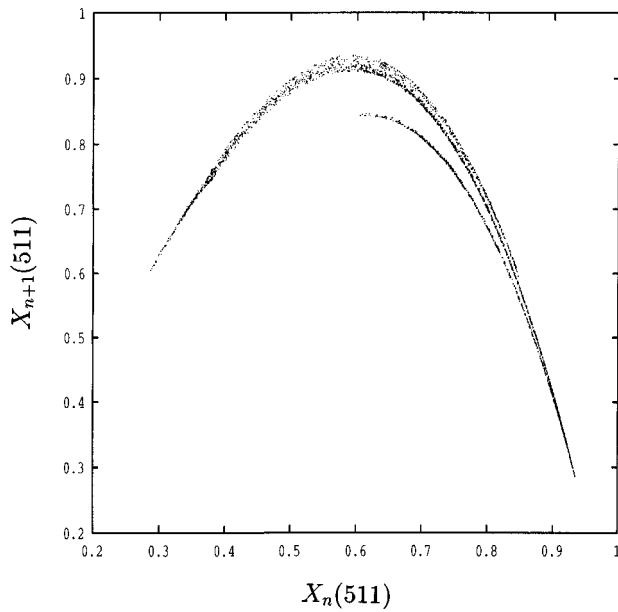


FIG. 5. A first return map for site $i=511$, $X_{n+1}(511)$ vs $X_n(511)$, with $D_0=2.9$ and $D=-3.0$. 3000 points have been plotted and 5000 iterations have been discarded as transient.

$D\partial^2 x_n(j)$, for $j=456$. From this diagram, we can see that due to the symmetry of the multiplicative diffusion coupled map lattices, Eq. (6), Fig. 6(b) is also symmetric about zero. The bifurcation structure of this figure is the same as Fig. 6(a). Therefore, we can conclude that the complex dynamics of the multiplicative diffusion coupled map lattices, when $D_0=2.9$, results from the term of diffusion, or the coupling equation (6).

B. Statistical property and spatial correlation

Furthermore, we have checked the fluctuations of the coupled map lattices for different system sizes. We consider the mean-square deviation (MSD) of the fluctuations of the mean field

$$MSD = \langle h_n^2 \rangle - \langle h_n \rangle^2, \tag{26}$$

where $h_n = (1/N) \sum_{j=1}^N f[x_n(j), D_n(x_n(j))]$ is the mean field. The reason to study these fluctuations is the following: when the system settles in a “turbulent” regime, its variables behave in a chaotic and seemingly uncoordinated way, and it may be possible that it mimics an ensemble of independent random variables. If this were so, then h_n should converge to a fixed value h^* as $N \rightarrow \infty$, with fluctuations around this limiting value normally distributed (Central Limit Theorem), and with a dispersion that decays as $1/\sqrt{N}$ (law of large numbers). That is, the mean-square deviation MSD would decrease as the system size N increases. In Fig. 7, we show the results for several different value of D . It shows that as the system size increases the mean-square deviation first decreases (except that of $D=-1.0$ which is independent on the system size N) and then it saturates as N increases. This implies that an ensemble of the maps does not have a statistical property.⁹ For the case of $D=-1.0$, because the dy-

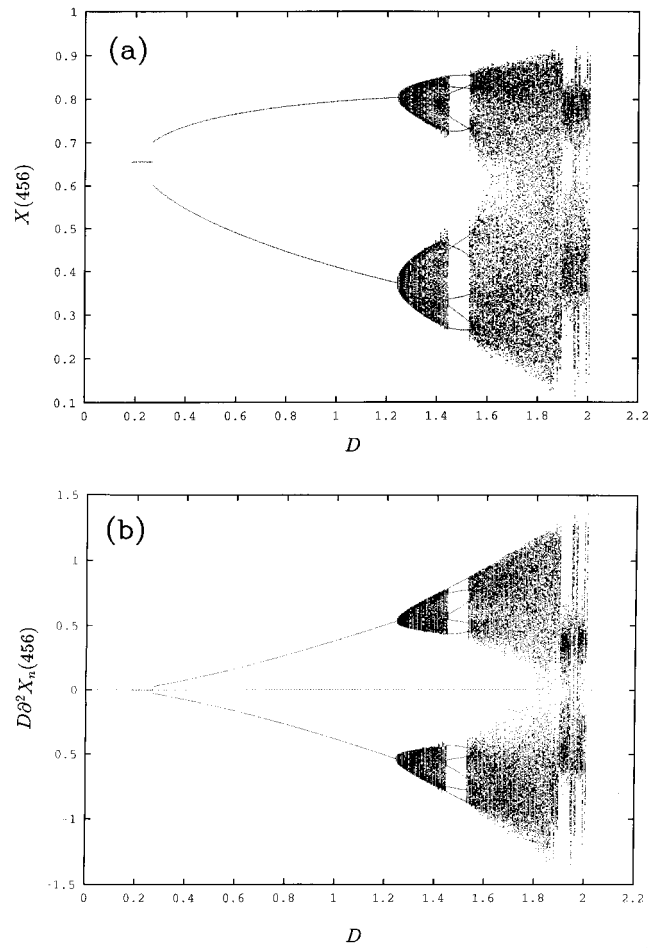


FIG. 6. Bifurcation diagrams for site $i=456$ and $D_0=2.9$ with (a): Eq. (8); (b): $D\partial^2 x_n(i)$. For each D value 200 points have been used and 5000 iterations have been discarded as transient. In (b), the dotted line in the middle is due to the software of the plotting.

namical state of the multiplicative diffusion coupled map lattices is a period-1 type and this state is not quasirandom, the result remains almost constant as N changes. It is noted that for Fig. 7, we have only used 50 runs for the statistical averaging for each value of D . If we use more runs, the curves are smoother, but the conclusion remains the same.

In usual coupled map lattices with a finite range of coupling, the law of large numbers is satisfied at the fully disordered state, because there exists a finite correlation length ξ , such that the spatial correlation decays as $\exp(-r/\xi)$.^{18,19} This is in contrast with the globally coupled case.²⁰ On the other hand, there are some examples showing the spatial order with temporal chaos, where the correlation does not decay; for instance, the pattern and domains in Ref. 21 belong to this class. In a system with a local spatial interaction, the breakdown of the law of large numbers implies the appearance of some kind of spatial orders.^{20,22} In our cases, for the frozen state, the correlation between the lattices is small because there are many zeros which block the correlation. Although within the small domains the lattice may be correlated together, the whole system is divided into many small subsystems and there are no correlations between them. The

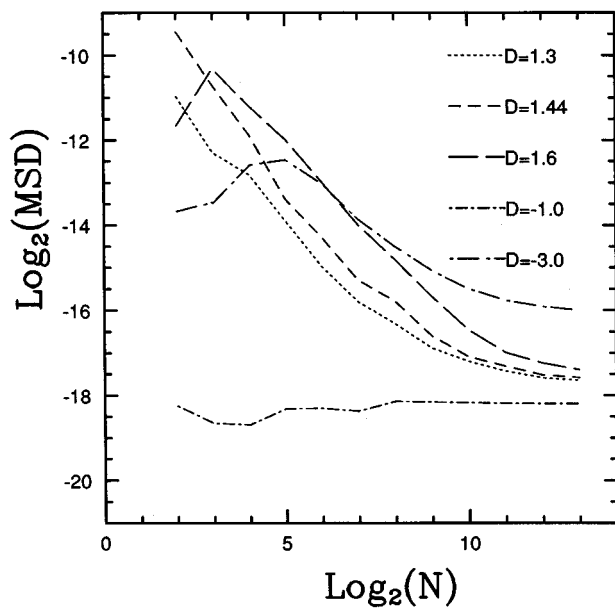


FIG. 7. Mean-square deviation of the mean field against system size N , $\log_2(\text{MSD})$ vs $\log_2(N)$, for five different D values. 50 runs have been used for the statistical averaging.

correlation is also very small for the homogeneous attractor since all the members of lattice converge to the fixed points. However, the situation will be different for the period-2 and chaotic states. There will be some correlations between the lattices for these two cases. The appearance of the period-2 and chaotic states is due to the strong correlation between the lattices.

In order to check the above arguments, we have calculated the spatial correlation function¹⁸

$$C(s) = \frac{1}{N_t N} \sum_{n=1}^{N_t} \sum_{j=1}^N [x_n(j+s) - \bar{x}_n][x_n(j) - \bar{x}_n], \quad (27)$$

where s is the distance between two spatial positions in the system and N_t is the total time steps and $\bar{x}_n = h_n$ is the mean field. In Fig. 8, we have shown the results of the correlation function $C(s)$ against s for several different values of D . For the case of $D = -3.0$, the correlation function is zero, $C(s) = 0$, which means the lattices have no correlations between each other [see curve (a) in Fig. 8], while it is very small when the diffusion coefficient $D = -1$ [curve (b) in Fig. 8]. These two cases show the situation we discussed above. From the other two curves [(c) and (d)] we can see that the correlation is a function of s . The correlation oscillates with a large amplitude for small distance, while it decays for large distance without losing its oscillatory behavior with a finite, but small, amplitude. Thus, the whole lattices do not evolve to a fully disordered state but to a weak chaotic or periodic one as we will discuss in the following section from the dynamical characterization by the Lyapunov exponents. There are some spatial orders in the system.

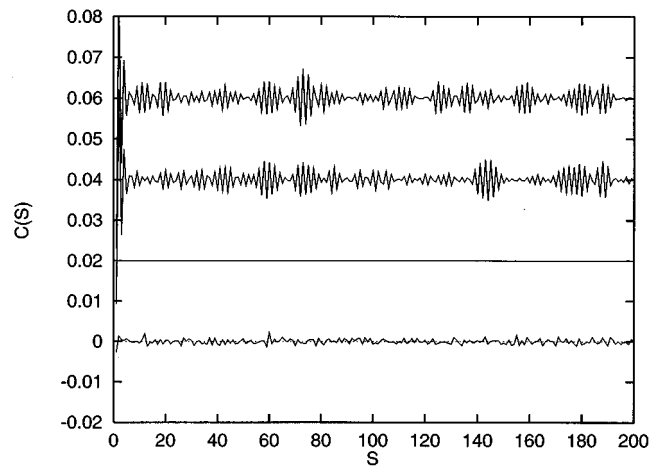


FIG. 8. The spatial correlation function $C(s)$ varying with the spatial separating distance s . 10 000 time steps were performed to eliminate transients, and then 10 000 steps have been taken for the average. From the bottom to the top with the values of D : (a) $D = -3.0$; (b) $D = -1.0$; (c) $D = 1.1$; (d) $D = 1.6$.

IV. DYNAMICAL CHARACTERIZATION

In order to characterize the above-mentioned spatiotemporal structures, we have also calculated the largest Lyapunov exponent of our map lattices.²³ We made such a calculation by considering that the state of the multiplicative diffusion coupled map lattices at time n is given by an N -dimensional vector

$$y_n = [x_n(1), x_n(2), \dots, x_n(N)]. \quad (28)$$

Then the sequence of states y_k for $k=0, 1, \dots$, is generated by the deterministic, discrete-time map, Eq. (8). We calculate the largest Lyapunov exponent Λ of this trajectory (the sequence) by using the method described in Ref. 24. In Fig. 9, we showed the largest Lyapunov exponent Λ against D . From this figure, we found an excellent agreement with the

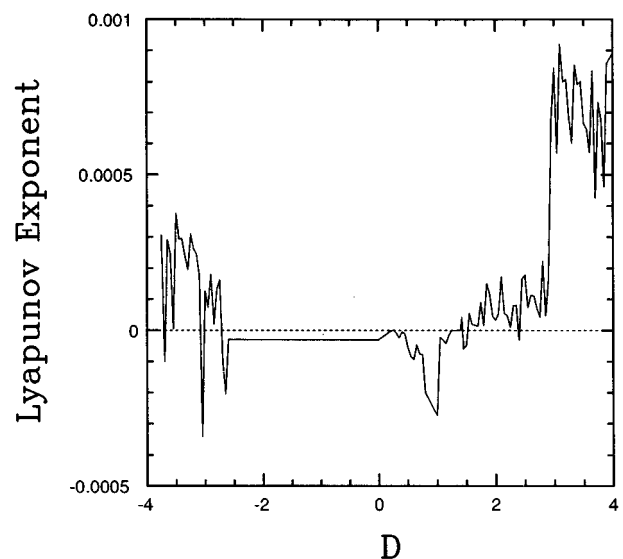


FIG. 9. The largest Lyapunov exponent Λ against D for $D_0 = 2.9$.

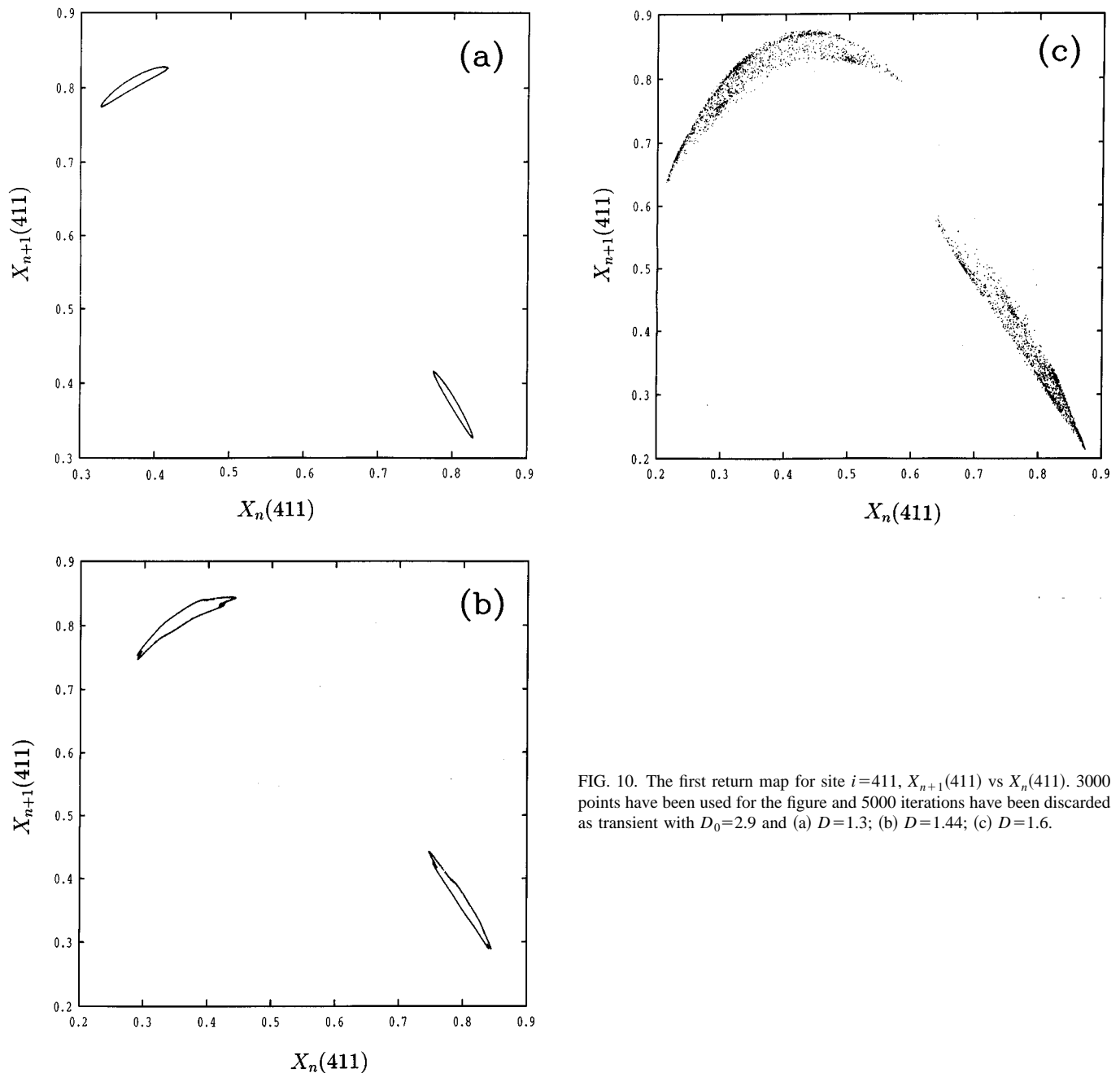


FIG. 10. The first return map for site $i=411$, $X_{n+1}(411)$ vs $X_n(411)$. 3000 points have been used for the figure and 5000 iterations have been discarded as transient with $D_0=2.9$ and (a) $D=1.3$; (b) $D=1.44$; (c) $D=1.6$.

above discussion. When $-2.64 < D < 1.215$, the largest Lyapunov exponent Λ is smaller than zero, $\Lambda < 0$, and the attractor corresponds to a period-1 state, i.e., the diffusive homogeneous state, and a period-2 state, respectively. For $1.215 < D < 1.42$, $\Lambda = 0$, the dynamical state of the multiplicative diffusion coupled map lattices is a quasiperiodic one. While $\Lambda > 0$ for $1.42 < D < 3.2$ and $-4.0 < D < -2.64$, with these D values the lattice has a chaotic behavior (except there are some periodic windows where $\Lambda < 0$). However, for $-4.0 < D < -2.64$ the state relates to a so-called “weak chaos” or local chaos for which some sites are chaotic and some sites frozen to be zero, as well as some sites that are still on the diffusive homogeneous attractor.

In Fig. 10, we showed the transition from a quasiperiodic to chaotic state for site $j=411$. We call these attractors (also Fig. 5) the local attractor or the first return map which is plotted by using $x_{n+1}(j)$ vs $x_n(j)$ for a certain site. However, under the same condition we have also seen that the local attractor of other site, say j th, is the same as that of the site i under equal iteration conditions (for those attractors with $D > -2.64$). For the quasiperiodic attractor, the points construct a continuous close curve while for the chaotic attractor there are some points out of the close curve or some points wrinkled together. To make sure this does not result from the transient, we have discarded very long iterations for these figures. From our previous discussion, we have seen

that the dynamical state is first a period-1 state. As D is increased, this period-1 state is unstable, and bifurcates into a period-2 state, and then develops into a quasiperiodic one [see Figs. 6 and 10(a)]. Furthermore, this quasiperiodic state evolves into a chaotic state when D is further increased [see Figs. 10(b) and 10(c)]. This chaotic behavior is clearly occurring via the transition from the quasiperiod. The route of the transition from quasiperiodicity to chaos may be the one described by Ruelle and Takens²⁵ which has been observed in many systems such as in fluid dynamics and also in our previous study for a coupled dissipative oscillator, a Josephson junction system, as in Ref. 26. However, a clear picture would be carried out by checking whether there is a Hopf bifurcation from a torus, which will be discussed in further work.

V. CONCLUSION

In the past, most of the work on chaotic dynamics has been concentrated on the temporal behavior of low-dimensional systems. Many physical systems of interest, however, as fluid flows, require the study of very high-dimensional systems which have intricate spatial and temporal evolution properties. Models which might reveal, therefore, some of the fundamental properties of spatially extended nonlinear systems are of great interest. Compared to partial differential equations they certainly have the drawback that they cannot in general be associated to realistic systems. But if one is interested in general mechanisms rather than in specific realizations, then they have the essential advantage of being much easier to simulate due to the discreteness in space and time. One such model is studied in this work.

In this work, we are interested in exploring the diffusive process of a model system from an initial random distribution and in finding the spatiotemporal structure. Actually, diffusive homogenization gives rise to numerous processes in solids, such as the onset of mechanical stresses, formation and growth of phases, chemical reactions, change of the electric conductivity, etc. These processes are usually described by using the macroscopic characteristics of the diffusive homogenization pictures, that is, the concentration profile and motion of plane having a constant concentration.

In conclusion, we presented a study of the multiplicative diffusion coupled map lattices with the coupling between the neighboring elements only through the bifurcation parameter of the mapping function in this paper. From an initially random distribution, we found that there are several types dynamics for the spatiotemporal structures of the lattice: (i) the diffusive homogeneous attractor, (ii) the frozen phenomenon, (iii) period-2 to chaotic state via quasiperiodic transition. We have discussed the dynamical and statistical behavior of the system for such structures. To characterize the dynamical behavior, we have used the largest Lyapunov exponent and the spatial correlation function for such a high-dimensional system.

It is worth comparing the multiplicative diffusion coupled map lattices with the “noisy” logistic map.²⁷ For

the latter case, the bifurcation parameter is $\mu = \mu_0 + \sigma$ for the logistic map $x_{n+1} = \mu x_n(1 - x_n)$. The noise makes that the bifurcation point widens and chaos appears only after two or three bifurcations. It has been shown by Sinha²⁸ that the effect of introducing parametric noise in an array of maps is twofold: when the maps are uncoupled, and fluctuations are spatiotemporal, i.e., the maps evolve under noise which varies randomly from site to site at every step of time, they observed statistical behavior in the mean field; on the other hand when all the elements are subjected to the same temporal random fluctuations, the mean field exhibits clear non-statistical behavior. Similarly, although the multiplicative diffusion coupled map lattices could be interpreted, in the chaotic region, as an array of maps with spatiotemporal parametric noise, our results also show nonstatistical behavior in the mean field. Therefore, it is completely different as we have seen above for the multiplicative diffusion coupled map lattices where the bifurcation parameter depends on a diffusive term related to the states of three sites within the lattice. It is this term that makes the dynamical behavior and the statistical behavior of such map lattices very different.

In addition, the self-modulated diffusive process within the multiplicative diffusion coupled map lattices shows a special frozen effect by which the system is divided into many domains. The appearance of these effects obeys a linear scaling with the diffusive parameter D . Within a domain, the dynamical state is either chaotic or fixed depending on how many lattices the domain has.

Finally, a more interesting extension of the present work might be to generalize it to two dimensions. We expect that the self-modulated diffusion process would result in some interesting patterns of the domain walls, and also the system can have a turbulent phase. It certainly deserves future study.

ACKNOWLEDGMENTS

We would like to thank Dr. G. Perez for valuable discussions. HAC acknowledges support from the Istituto Nazionale de Fisica Nucleare (INFN). WW thanks the partial support provided by a Ke-Li Fellowship and the Young Research Foundation of the Committee of National Education.

¹A. R. Bishop, K. Fesser, P. S. Lomdahl, W. C. Kerr, M. B. Williams, and S. E. Trullinger, *Phys. Rev. Lett.* **50**, 1095 (1983).

²Y. Kuramoto and S. Koga, *Prog. Theor. Phys.* **66**, 1081 (1981);

³A. Arueodo, P. Couillet, C. Tresser, A. Libchaber, J. Maurer, and D. d’Humieres, *Physica D* **6**, 386 (1983).

⁴A. R. Bishop, G. Gruner, and B. Nicolaenko (editors), *Spatio-temporal Coherence and Chaos in Physical Systems*, *Physica D* **23** (1986).

⁵T. Bohr, G. Grinstein, Y. He, and C. Jayaprakash, *Phys. Rev. Lett.* **58**, 2155 (1987).

⁶K. Kaneko, *Physica D* **37**, 60 (1989).

⁷K. Kaneko, *Physica D* **41**, 137 (1990).

⁸M. H. Jensen, *Phys. Scr.* **T38**, 22 (1991).

⁹G. Perez, S. Sinha, and H. A. Cerdeira, *Physica D* **63**, 341 (1993).

¹⁰A. T. Winfree, “The geometry of biological time,” in *Biomathematics* (Springer-Verlag, Berlin, 1990), Vol. 8.

¹¹J. P. Crutchfield and K. Kaneko, “Phenomenology of spatio-temporal chaos,” in *Directors in Chaos*, edited by H. Bai-lin (World Scientific Singapore, 1987).

¹²P. Grassberger and T. Schreiber, *Physica D* **50**, 177 (1991).

¹³S. Puri, R. C. Desai, and R. Kapral, *Physica D* **50**, 207 (1991).

- ¹⁴T. S. Akhromeyeva, S. P. Kurdyumov, G. G. Malinetskii, and A. A. Samarskii, *Phys. Rep.* **176**, 189 (1989).
- ¹⁵O. A. Druzhinin and A. S. Mikhailov, *Phys. Lett. A* **148**, 429 (1990).
- ¹⁶J. S. Langer, *Rev. Mod. Phys.* **52**, 1 (1980).
- ¹⁷E. Ben-Jacob, H. Shmueli, O. Shochet, and A. Tenenbaum, *Physica A* **187**, 378 (1992).
- ¹⁸F. Kasper and H. G. Schuster, *Phys. Lett. A* **113**, 451 (1986).
- ¹⁹D. R. Rasmussen and T. Bohr, *Phys. Lett. A* **125**, 107 (1987).
- ²⁰K. Kaneko, *Phys. Rev. Lett.* **65**, 1391 (1990).
- ²¹K. Kaneko, *Physica D* **34**, 1 (1989).
- ²²K. Kaneko, *Physica D* **55**, 368 (1992).
- ²³Here in this work we did not use the conventional Jacobi matrices algorithm for the Lyapunov exponent since we want to extend our study to a more general case of the differential equations with the diffusion mechanism. But we have checked that both methods give the same results for the present coupled map lattices.
- ²⁴L. F. Olsen and H. Degn, "Chaos in biological systems," in *Chaos II*, edited by H. Bai-lin (World Scientific, Singapore, 1990).
- ²⁵D. Ruelle and F. Takens, *Commun. Math. Phys.* **20**, 167 (1971).
- ²⁶W. Wang, A. L. Thomson, and X. Yao, *Phys. Rev. B* **44**, 4618 (1991).
- ²⁷J. P. Crutchfield, J. D. Farmer, and B. A. Huberman, *Phys. Rep.* **92**, 45 (1982).
- ²⁸S. Sinha, *Phys. Rev. Lett.* **69**, 3306 (1992).